LETTER

doi:10.1038/nature10181

Protein targeting and degradation are coupled for elimination of mislocalized proteins

Tara Hessa[1], Ajay Sharma[1], Malaiyalam Mariappan[1], Heather D. Eshleman[1]†, Erik Gutierrez[1,2] & Ramanujan S. Hegde[1]†

A substantial proportion of the genome encodes membrane proteins that are delivered to the endoplasmic reticulum by dedicated targeting pathways[1]. Membrane proteins that fail targeting must be rapidly degraded to avoid aggregation and disruption of cytosolic protein homeostasis[2,3]. The mechanisms of mislocalized protein (MLP) degradation are unknown. Here we reconstitute MLP degradation *in vitro* to identify factors involved in this pathway. We find that nascent membrane proteins tethered to ribosomes are not substrates for ubiquitination unless they are released into the cytosol. Their inappropriate release results in capture by the Bag6 complex, a recently identified ribosome-associating chaperone[4]. Bag6-complex-mediated capture depends on the presence of unprocessed or non-inserted hydrophobic domains that distinguish MLPs from potential cytosolic proteins. A subset of these Bag6 complex 'clients' are transferred to TRC40 for insertion into the membrane, whereas the remainder are rapidly ubiquitinated. Depletion of the Bag6 complex selectively impairs the efficient ubiquitination of MLPs. Thus, by its presence on ribosomes that are synthesizing nascent membrane proteins, the Bag6 complex links targeting and ubiquitination pathways. We propose that such coupling allows the fast tracking of MLPs for degradation without futile engagement of the cytosolic folding machinery.

Protein targeting and translocation to the endoplasmic reticulum (ER) are not perfectly efficient[5,6], thereby necessitating pathways for the degradation of MLPs that have been inappropriately released into the cytosol. For example, mammalian prion protein (PrP), a widely expressed glycosyl phosphatidylinositol (GPI)-anchored cell surface glycoprotein, displays ~5–15% translocation failure *in vitro* and *in vivo*[2,3,5–10]. This non-translocated population of PrP is degraded efficiently by a proteasome-dependent pathway, limiting the cytosolic PrP levels at steady state[2,3,9,10]. Prompt degradation is essential because mislocalized PrP can aggregate, make inappropriate interactions, and cause cell death and neurodegeneration[2,11–14]. The pathways for efficient disposal of MLPs, however, are not known.

To study this problem, we reconstituted the ubiquitination of mislocalized PrP *in vitro*. Radiolabelled PrP synthesized in rabbit reticulocyte lysate (RRL) supplemented with ER-derived rough microsomes was predominantly translocated into the ER, processed and glycosylated (Fig. 1a). However, various conditions that reduced the extent of translocation—such as omission of rough microsomes, inactivation of signal recognition particle (SRP)-dependent targeting or blocking of translocation through the translocon—all resulted in increased PrP ubiquitination in a lysine-dependent manner (Fig. 1a and Supplementary Figs 1–3). Other mislocalized secretory and membrane proteins were also similarly ubiquitinated in the cytosol (Supplementary Fig. 4). The ubiquitination of mislocalized PrP closely parallels PrP synthesis (Fig. 1b), suggesting that ubiquitination is rapid. Yet, ubiquitination occurred strictly post-translationally, because full-length PrP that was tethered as a nascent peptidyl-transfer RNA to the ribosome was not ubiquitinated until it had been released into the cytosol through the action of puromycin (Fig. 1c and Supplementary Fig. 5). An unrelated membrane protein behaved similarly (Supplementary Fig. 6).

Efficient ubiquitination of PrP was strongly dependent on unprocessed hydrophobic signals at the amino and carboxy termini (Fig. 1d). Conversely, green fluorescent protein (GFP) became a substrate for ubiquitination when hydrophobic targeting signals were added (Supplementary Fig. 4). Ubiquitination was therefore not solely a consequence of protein misfolding, because PrP lacking both the N-terminal targeting signal (denoted ΔSS) and the C-terminal GPI-anchoring signal (ΔGPI) was misfolded owing to its lack of glycosylation and disulphide bond formation, but was poorly ubiquitinated. This finding suggested the existence of a specialized pathway for hydrophobic-domain-containing MLPs that works more rapidly than traditional quality control pathways, which engage only after repeated failures at folding[15,16].

To identify factors involved in the MLP degradation pathway, we combined biochemical fractionation and functional reconstitution assays. We produced a translation-competent fractionated RRL (Fr-RRL) (Supplementary Fig. 7) that selectively decreased the ubiquitination of non-translocated PrP (Fig. 2a) and other MLPs (Supplementary

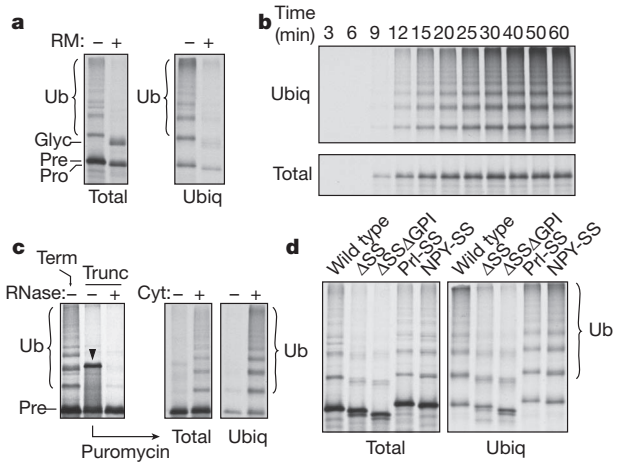

Figure 1 | Non-translocated PrP is rapidly ubiquitinated. a, The translation of radiolabelled PrP in RRL, with or without rough microsomes (RMs), was analysed directly (left) or after isolation of ubiquitinated (ubiq) products (right) by using SDS–PAGE and autoradiography. Glycosylated (glyc), precursor (pre), processed (pro) and ubiquitinated (Ub) bands are indicated. **b**, Time course of PrP synthesis (bottom) and PrP ubiquitination (top) *in vitro*. **c**, PrP containing a termination codon (term) or lacking this codon (trunc) was translated *in vitro*. Truncated PrP was released using puromycin, in the absence or presence of cytosol (cyt), and total protein and ubiquitination were analysed. The arrowhead indicates tRNA-containing PrP, which can be digested by RNase. **d**, Wild-type PrP or constructs lacking the signal sequence (ΔSS) or both the signal sequence and GPI anchor (ΔSSΔGPI) were analysed directly or after isolation of ubiquitinated products. Prl-SS and NYP-SS contain signal sequence from preprolactin and neuropeptide Y, respectively.

[1]Cell Biology and Metabolism Program, National Institute of Child Health and Human Development, National Institutes of Health, Bethesda, Maryland 20892, USA. [2]Department of Biology, Johns Hopkins University, Baltimore, Maryland 21218, USA. †Present addresses: Department of Physiology, University of California, San Francisco, California 94158, USA (H.D.E.); MRC Laboratory of Molecular Biology, Hills Road, Cambridge CB2 0QH, UK (R.S.H.).

Fig. 8) but not ubiquitination in general (Supplementary Fig. 7). The missing factor in Fr-RRL (other than ubiquitin, which we included in all assays) proved to be the E2 ubiquitin-conjugating enzyme UBCH5 (also known as UBE2D1) (Fig. 2b and Supplementary Figs 8 and 9). Because UBCH5 restored ubiquitination equally well when added during or after PrP translation (Fig. 2b), we surmised that at least a certain population of PrP remains in a ubiquitination-competent state. Indeed, PrP and other MLPs that were affinity purified from Fr-RRL under native conditions could be ubiquitinated simply by adding purified E1, UBCH5, ubiquitin and ATP (Fig. 2c and Supplementary Fig. 10).

To identify factors that maintain the ubiquitination competence of MLPs, the Fr-RRL translation products were separated by size in a sucrose gradient, and each fraction was subjected to parallel ubiquitination and chemical crosslinking analyses (Fig. 2d and Supplementary Fig. 11). The fractions retaining maximum ubiquitination competence for two different substrates correlated well with a ~150-kDa crosslinking partner (Fig. 2d and Supplementary Fig. 11). This interaction was direct (Supplementary Fig. 12) and was strongly dependent on the presence of unprocessed N- and C-terminal signals in PrP (Fig. 2e and Supplementary Fig. 13), correlating with the requirements for ubiquitination (Fig. 1d). On the basis of molecular weight, dependence on hydrophobic domains for interaction and migration position in the sucrose gradient, we surmised that the ~150-kDa crosslinked protein might be BAG6 (also called BAT3 and Scythe), a hypothesis that was subsequently verified by immunoprecipitation experiments (Fig. 2e and Supplementary Figs 13 and 14). BAG6 was recently identified as part of a three-protein ribosome-interacting chaperone complex (composed of BAG6, TRC35 and UBL4A)[4] that is involved in tail-anchored membrane-protein insertion into the ER[4,17]. A combination of crosslinking, affinity purification and immunoblotting studies verified that all three subunits of this complex are associated with MLPs

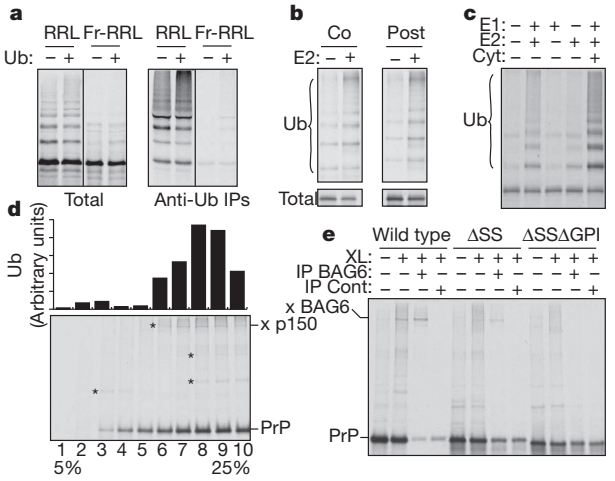

Figure 2 | BAG6 interacts with MLPs through hydrophobic domains. **a**, PrP translated in RRL or Fr-RRL, with or without 10 μM ubiquitin (Ub), was analysed directly (left) or after anti-ubiquitin antibody immunoprecipitation (IP) (right) by using SDS–PAGE and autoradiography. **b**, PrP translated in Fr-RRL was ubiquitinated when UBCH5 (E2; 250 nM) was included co-translationally (co) or post-translationally (post). Total synthesis (bottom) and ubiquitinated products (top) are shown. **c**, PrP was immunoaffinity purified under native conditions and incubated with the indicated components (cyt, cytosol; E1 enzyme, 100 nM; E2 enzyme, UBCH5, 250 nM). All reactions contained His–ubiquitin and ATP. Purified ubiquitinated products are shown. **d**, PrP translated in Fr-RRL was separated into ten fractions in a 5–25% sucrose gradient. The fractions were subjected to chemical crosslinking (bottom) or ubiquitination assays (top). Asterisks indicate crosslinks. Histogram bars indicate the amount of ubiquitinated product in each fraction. The ~150-kDa crosslinking partner (x p150) is indicated. **e**, Crosslinking reactions (XL) of *in vitro*-synthesized PrP or PrP deletion constructs were analysed directly or after immunoprecipitation with anti-BAG6 or control (cont) antibodies. The crosslink to BAG6 (x BAG6) is indicated.

(Supplementary Figs 14 and 15, and data not shown). Thus, the Bag6 complex binds to multiple MLPs through their hydrophobic domains and has a broader specificity than only binding tail-anchored proteins.

To determine when the Bag6 complex first captures MLPs, we analysed ribosome-nascent chains (RNCs) of membrane proteins. When a transmembrane domain (TMD) emerged from the ribosomal 'tunnel', a direct interaction with SRP54 (the signal-sequence-binding subunit of the SRP) was detected by crosslinking experiments (Fig. 3a–c). By contrast, the Bag6 complex, even though it has been found to reside on such RNCs and is abundant in the cytosol[4], did not make direct contact with the substrate (Fig. 3b, c). When the TMD was still inside the ribosomal tunnel, the RNC was not crosslinked to either BAG6 or SRP54 (Fig. 3c), even though both complexes can be recruited to such ribosomes[4,18]. After puromycin release of each of these RNCs (with the TMD inside versus outside the ribosomal tunnel), BAG6 crosslinking was observed (Fig. 3b, c). Thus, the Bag6 complex captures substrates concomitant with or after the release of nascent chains from the ribosome; these same hydrophobic domains are bound by the SRP as long as the TMD is exposed as an RNC[19].

Earlier analysis of tail-anchored and non-tail-anchored membrane proteins had shown that only tail-anchored membrane proteins are efficiently loaded onto TRC40 (also known as ASNA1), the targeting factor for tail-anchored protein insertion into the ER[20]. Indeed, modifying a tail-anchored protein either by placing cyan fluorescent protein (CFP) polypeptide sequences after the TMD (a construct denoted β-CFP) (Fig. 3a) or by adding an extra TMD (denoted TR-β) reduced the interactions with TRC40 and simultaneously increased the interactions with the Bag6 complex (Fig. 3d). Similarly, comparison of the crosslinking partners of PrP and those of the tail-anchored protein Sec61β showed that both of these proteins interact with the Bag6 complex, but only Sec61β is primarily found bound to TRC40 (Supplementary Fig. 15). Given that the loading of tail-anchored proteins onto TRC40 depends on the Bag6 complex[4], these data suggest that the Bag6 complex is acting as a triage

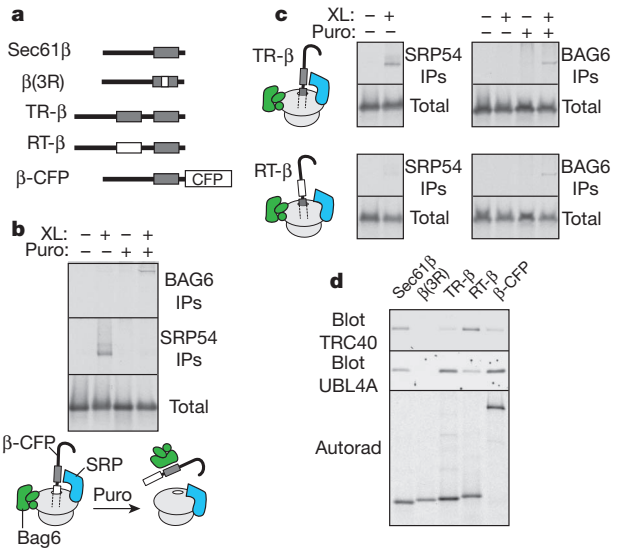

Figure 3 | BAG6 captures MLPs released from the ribosome. **a**, Diagram of constructs derived from Sec61β, with transmembrane domains shown as grey boxes and hydrophilic changes in white boxes. **b**, RNCs of β-CFP with the TMD outside the ribosome were subjected to crosslinking (XL) before or after release by puromycin (puro) and were analysed directly (bottom) or after immunoprecipitation (IP) with anti-BAG6 antibody (top) or anti-SRP54 antibody (centre). The results are also illustrated diagrammatically: Bag6 complex, green; SRP, blue; and ribosome, pale grey. **c**, The assays were as described in **b** but using TR-β (top) and RT-β (bottom). **d**, The indicated constructs were translated *in vitro*, immunoaffinity purified through their N terminus, and immunoblotted with anti-TRC40 antibody or anti-UBL4A antibody (the latter to detect the Bag6 complex). The autoradiograph shows equal recovery of the translated substrates.

factor: that is, it captures a relatively broad range of membrane proteins after their ribosomal release but transfers only a subset of them (namely, tail-anchored proteins) to TRC40 for post-translational membrane insertion. The remainder seem to be targeted for ubiquitination because of their persistent interaction with BAG6.

To examine this hypothesis, we immunodepleted the Bag6 complex from RRL (Supplementary Fig. 16) and found that the ubiquitination of several MLPs was reduced (Fig. 4a and Supplementary Fig. 17). By contrast, the control protein GFP was not ubiquitinated in RRL but became a substrate when it was attached to either a ubiquitin molecule or any of several hydrophobic ER-targeting domains (Supplementary Fig. 18). Only the hydrophobically modified GFP proteins were BAG6 dependent in their ubiquitination, consistent with their interaction with BAG6 by crosslinking analysis (Supplementary Fig. 13). Conversely, ΔSSΔGPI-PrP, which does not interact with BAG6 (Fig. 2e), was ubiquitinated (albeit slowly and less efficiently) in a BAG6-independent manner (Fig. 4a). Disrupting the TMD of Sec61β with three arginine residues (denoted β(3R)), which disrupts BAG6 interaction[4], also resulted in less ubiquitination, which was no longer BAG6 dependent (Fig. 4a). Thus, the Bag6 complex is not required for ubiquitination of all misfolded proteins but is especially important for the efficient ubiquitination of MLPs.

When recombinant BAG6 (Supplementary Fig. 16) was added to translation extracts that had been depleted of the Bag6 complex, the ubiquitination of a model MLP was restored (Fig. 4b), and the recombinant BAG6 interacted with this MLP in crosslinking assays (Fig. 4c).

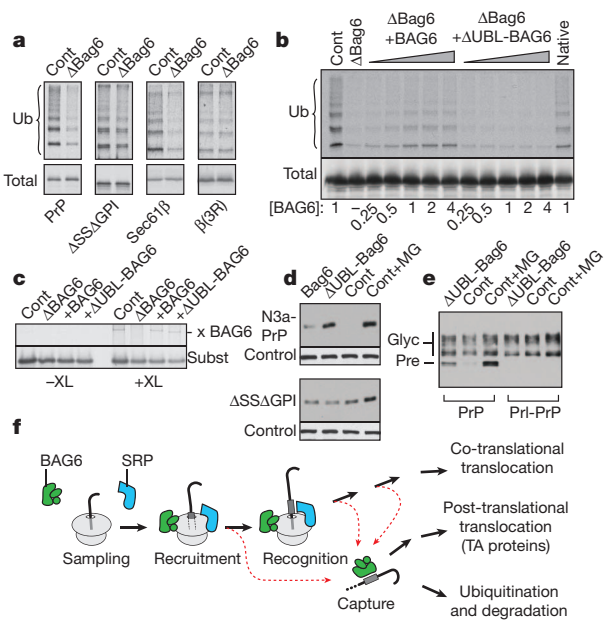

Figure 4 | Maximum ubiquitination of MLPs requires BAG6. **a**, Various constructs (listed at bottom) were assayed for ubiquitination in lysates containing Bag6 complex (control, cont) or lacking Bag6 complex (ΔBag6). The gels for assessing ubiquitination for the ΔSSΔGPI and β(3R) constructs were exposed about threefold longer than those for PrP and Sec61β. **b**, Bag6-complex-depleted lysates (ΔBag6) were replenished with increasing amounts (wedges) of recombinant BAG6 (Supplementary Fig. 16), ΔUBL-BAG6 or native Bag6 complex and then analysed for the ubiquitination of TR-β. Relative BAG6 levels are indicated (listed at bottom). **c**, TR-β interacts with recombinant BAG6 and ΔUBL-BAG6 by crosslinking (XL). Subst, substrate; x BAG6, crosslink to BAG6. **d**, The indicated PrP constructs (N3a-PrP and ΔSSΔGPI) were co-transfected with Bag6 complex, ΔUBL-Bag6 complex or control plasmid (cont) (Supplementary Fig. 20), and PrP was detected by immunoblotting. One sample was treated with the proteasome inhibitor MG132 (MG) for 4 h. A loading control (control) is also shown. **e**, Effect of the ΔUBL-Bag6 complex on wild-type PrP and Prl-PrP. Unglycosylated precursor PrP (pre) is preferentially stabilized by either overexpression of the ΔUBL-Bag6 complex or inhibition of the proteasome. **f**, The model we propose is that the Bag6 complex captures ribosomally released hydrophobic proteins (red arrows) and triages them between post-translational targeting (for tail-anchored (TA) proteins) and ubiquitination.

BAG6 lacking its N-terminal UBL domain (ΔUBL-BAG6) was inactive in restoring ubiquitination (Fig. 4b) despite interacting normally with substrate (Fig. 4c). This finding suggested that BAG6 may recruit the ubiquitination machinery to substrates through its UBL domain. To test this, Flag-tagged recombinant BAG6 or ΔUBL-BAG6 was added to the Fr-RRL translation system lacking the E2 enzyme UBCH5 (Supplementary Fig. 7). BAG6–substrate complexes were immunopurified through the Flag tag and incubated with purified E1 ubiquitin-activating enzyme, E2 enzyme, ubiquitin and ATP. Substrate ubiquitination was observed with BAG6 but not ΔUBL-BAG6, verifying that the UBL domain recruits the ubiquitination machinery to the substrate (Supplementary Fig. 19). Indeed, BAG6 has been observed to interact with E3 ubiquitin ligases through its UBL domain[21,28].

In Fig. 4b, c, the data indicated that ΔUBL-BAG6 should act as a dominant negative and partly stabilize BAG6 substrates, thereby providing a selective tool for *in vivo* analysis. We therefore overexpressed the Bag6 complex or the ΔUBL-Bag6 complex (by about twofold) (Supplementary Fig. 20) in cultured cells and assessed the levels of a co-expressed MLP substrate. A translocation-impaired signal-sequence mutant of PrP (termed N3a-PrP)[5] was stabilized by the ΔUBL-Bag6 complex but almost unaffected by the wild-type Bag6 complex (Fig. 4d). Importantly, ΔSSΔGPI-PrP, which does not interact with BAG6 (Fig. 2e), was unaffected by either Bag6 complex or ΔUBL-Bag6 complex overexpression (Fig. 4d) and showed higher steady-state levels than N3a-PrP (data not shown). This finding suggests that degradation is occurring by a different quality control pathway, consistent with the failure of ΔSSΔGPI-PrP to be recognized as an MLP (Fig. 2e).

Wild-type PrP, the translocation of which is slightly inefficient *in vivo*[2,3,6,8–10], showed preferential stabilization of a non-glycosylated species when co-overexpressed with ΔUBL-Bag6 complexes (Fig. 4e and Supplementary Fig. 21). This species was stabilized by proteasome inhibition and had been shown in earlier studies to be a non-translocated PrP precursor[2,3,9,10]. Replacing the slightly inefficient PrP signal sequence with the efficient signal from preprolactin (Prl-PrP) precluded the generation of non-glycosylated PrP with either proteasome inhibition or ΔUBL-Bag6 complex overexpression (Fig. 4e). Although the extent of stabilization seems modest, it is comparable to that seen after 2 h proteasome inhibition (Supplementary Fig. 21). Partial knockdown of BAG6 with a short hairpin RNA (shRNA) similarly stabilized a non-glycosylated species of PrP (Supplementary Fig. 22). Thus, MLPs are not only generated *in vivo*[2,3,6,8–10], but also require functional BAG6 for maximally efficient degradation.

Our results reveal a pathway for MLP degradation and identify an unexpectedly close link with protein targeting (Fig. 4f). Ribosomes synthesizing nascent membrane proteins can recruit both the SRP and Bag6 complex on entry of the first hydrophobic segment into the ribosomal tunnel[4,18]. This is a potential targeting complex for the ER membrane in both the co-translational and post-translational membrane-protein insertion pathways. We now find that such ribosomes are also potential degradation complexes because the first component of this degradation pathway is already poised to act in the event of failed targeting or inappropriate release from the ribosome. BAG6 therefore imposes a degradative fate on membrane proteins that can be avoided only by productive targeting.

Because membrane proteins would never fold in the cytosol, their direct degradation by a specialized pathway may be important to avoid unnecessarily occupying essential cellular folding pathways, particularly under conditions of stress. MLPs are distinguished from nascent cytosolic proteins by relatively long linear hydrophobic stretches, a feature that is important for BAG6 recognition. Indeed, mutagenesis shows that even modest reductions of TMD hydrophobicity sharply curtail BAG6 interaction[4]. This specificity distinguishes BAG6 from more general chaperones such as heat-shock protein 70 (HSP70), the substrate-binding pocket of which seems more suited to the shorter, moderately hydrophobic segments that typify nascent cytosolic proteins. This differential specificity probably explains how MLPs are triaged differently from other

potential substrates of cytosolic quality control[15,16,22–28]. These pathways could intersect or cooperate in as yet undefined ways given that BAG6 and HSP70 have been observed to co-immunoprecipitate[26].

In addition to this role in degradation, the Bag6 complex also facilitates the loading of tail-anchored proteins onto TRC40 for post-translational insertion into the ER[4]. As expected, tail-anchored proteins were also ubiquitinated by way of BAG6 in the absence of, or saturation of, TRC40 (Supplementary Fig. 23). Thus, substrates of both the co-translational and post-translational targeting pathways are ubiquitinated in a BAG6-dependent manner when targeting fails. After ubiquitination, BAG6 might chaperone its polyubiquitinated substrates to the proteasome, a function that was recently proposed on the basis of the co-immunoprecipitation of BAG6 with polyubiquitinated proteins[26]. The Bag6 complex is therefore a multi-purpose triage factor for chaperoning especially hydrophobic proteins through the aqueous cytosol. This view conceptually links its roles in tail-anchored protein targeting[4,17], in the MLP pathway (in this study), as a chaperone for newly dislocated proteins during ER-associated protein degradation[27,28] and in the delivery of terminally misfolded proteins to the proteasome[26].

METHODS SUMMARY

Reagents and standard methods. The plasmids and antibodies used and the assays carried out (*in vitro* translation assays, sucrose gradient separations, chemical crosslinking analyses, immunoprecipitation assays and immunodepletion assays) were as previously described[2–8,14,20,29,30]. Pull-down assays with Co^{2+} immobilized on chelating sepharose were performed on samples that had been denatured in boiling 1% SDS and then diluted tenfold in 4 °C pull-down buffer: 0.5% Triton X-100, 25 mM HEPES, 100 mM NaCl and 10 mM imidazole. Culture, transfection and immunoblotting analysis of N2a cells (dominant-negative inhibition experiments) and HeLa cells (for shRNA experiments) were carried out as previously described[2,3]. Full-length BAG6 (or ΔUBL-BAG6, which lacks residues 15–89) tagged at the C terminus with a Flag epitope was overexpressed after transient transfection of HEK-293T cells and then purified with anti-Flag resin under high salt (400 mM potassium acetate) conditions.

Modified translation extracts. Fr-RRL contained native ribosomes (isolated from RRL) mixed with a diethylaminoethyl (DEAE) sepharose ion-exchange chromatography elution fraction prepared from ribosome-free RRL (Supplementary Fig. 7). Fr-RRL was adjusted to the following final conditions for translation: 72 mM potassium acetate, 2.5 mM magnesium acetate, 10 mM HEPES, pH 7.4, 2 mM dithiothreitol (DTT), 0.2 mg ml^{-1} liver transfer RNA, 1 mM ATP, 1 mM GTP, 12 mM creatine phosphate, 40 μg ml^{-1} creatine kinase, 40 μM each amino acid (except methionine) and 1 μCi μl^{-1} [^{35}S]methionine.

Ubiquitination assays. For full-length proteins, translations containing 10 μM His-tagged ubiquitin were carried out for 1 h at 32 °C. In Fr-RRL, post-translational ubiquitination was initiated by adding E2 enzyme to a final concentration of 250 nM and incubating for 1 h at 32 °C. For RNCs, samples were supplemented with E1 enzyme (85 nM), E2 enzyme (usually 250 nM or 500 nM), cytosol (RRL or Fr-RRL), 10 μM His–ubiquitin, an ATP-regenerating system (1 mM ATP, 10 mM creatine phosphate and 40 μg ml^{-1} creatine kinase) and 1 mM puromycin. The reaction conditions were 100 mM potassium acetate, 50 mM HEPES, pH 7.4, 5 mM $MgCl_2$ and 1 mM DTT. Incubations were carried out for 1 h at 32 °C. On-bead ubiquitination of affinity-purified products was carried out under the same conditions, except without the inclusion of puromycin.

Full Methods and any associated references are available in the online version of the paper at www.nature.com/nature.

Received 8 December 2010; accepted 6 May 2011.
Published online 10 July 2011.

1. Cross, B. C., Sinning, I., Luirink, J. & High, S. Delivering proteins for export from the cytosol. *Nature Rev. Mol. Cell Biol.* **10,** 255–264 (2009).
2. Rane, N. S., Yonkovich, J. L. & Hegde, R. S. Protection from cytosolic prion protein toxicity by modulation of protein translocation. *EMBO J.* **23,** 4550–4559 (2004).
3. Kang, S. W. *et al.* Substrate-specific translocational attenuation during ER stress defines a pre-emptive quality control pathway. *Cell* **127,** 999–1013 (2006).
4. Mariappan, M. *et al.* A ribosome-associating factor chaperones tail-anchored membrane proteins. *Nature* **466,** 1120–1124 (2010).
5. Kim, S. J., Mitra, D., Salerno, J. R. & Hegde, R. S. Signal sequences control gating of the protein translocation channel in a substrate-specific manner. *Dev. Cell* **2,** 207–217 (2002).
6. Levine, C. G., Mitra, D., Sharma, A., Smith, C. L. & Hegde, R. S. The efficiency of protein compartmentalization into the secretory pathway. *Mol. Biol. Cell* **16,** 279–291 (2005).
7. Kim, S. J. & Hegde, R. S. Cotranslational partitioning of nascent prion protein into multiple populations at the translocation channel. *Mol. Biol. Cell* **13,** 3775–3786 (2002).
8. Rane, N. S., Chakrabarti, O., Feigenbaum, L. & Hegde, R. S. Signal sequence insufficiency contributes to neurodegeneration caused by transmembrane prion protein. *J. Cell Biol.* **188,** 515–526 (2010).
9. Orsi, A., Fioriti, L., Chiesa, R. & Sitia, R. Conditions of endoplasmic reticulum stress favor the accumulation of cytosolic prion protein. *J. Biol. Chem.* **281,** 30431–30438 (2006).
10. Drisaldi, B. *et al.* Mutant PrP is delayed in its exit from the endoplasmic reticulum, but neither wild-type nor mutant PrP undergoes retrotranslocation prior to proteasomal degradation. *J. Biol. Chem.* **278,** 21732–21743 (2003).
11. Ma, J. & Lindquist, S. Conversion of PrP to a self-perpetuating PrPSc-like conformation in the cytosol. *Science* **298,** 1785–1788 (2002).
12. Chakrabarti, O. & Hegde, R. S. Functional depletion of mahogunin by cytosolically exposed prion protein contributes to neurodegeneration. *Cell* **137,** 1136–1147 (2009).
13. Ma, J., Wollmann, R. & Lindquist, S. Neurotoxicity and neurodegeneration when PrP accumulates in the cytosol. *Science* **298,** 1781–1785 (2002).
14. Rane, N. S., Kang, S. W., Chakrabarti, O., Feigenbaum, L. & Hegde, R. S. Reduced translocation of nascent prion protein during ER stress contributes to neurodegeneration. *Dev. Cell* **15,** 359–370 (2008).
15. Buchberger, A., Bukau, B. & Sommer, T. Protein quality control in the cytosol and the endoplasmic reticulum: brothers in arms. *Mol. Cell* **40,** 238–252 (2010).
16. McDonough, H. & Patterson, C. CHIP: a link between the chaperone and proteasome systems. *Cell Stress Chaperones* **8,** 303–308 (2003).
17. Leznicki, P., Clancy, A., Schwappach, B. & High, S. Bat3 promotes the membrane integration of tail-anchored proteins. *J. Cell Sci.* **123,** 2170–2178 (2010).
18. Berndt, U., Oellerer, S., Zhang, Y., Johnson, A. E. & Rospert, S. A signal-anchor sequence stimulates signal recognition particle binding to ribosomes from inside the exit tunnel. *Proc. Natl Acad. Sci. USA* **106,** 1398–1403 (2009).
19. Keenan, R. J., Freymann, D. M., Stroud, R. M. & Walter, P. The signal recognition particle. *Annu. Rev. Biochem.* **70,** 755–775 (2001).
20. Stefanovic, S. & Hegde, R. S. Identification of a targeting factor for posttranslational membrane protein insertion into the ER. *Cell* **128,** 1147–1159 (2007).
21. Lehner, B. *et al.* Analysis of a high-throughput yeast two-hybrid system and its use to predict the function of intracellular proteins encoded within the human MHC class III region. *Genomics* **83,** 153–167 (2004).
22. Park, S. H. *et al.* The cytoplasmic Hsp70 chaperone machinery subjects misfolded and endoplasmic reticulum import-incompetent proteins to degradation via the ubiquitin–proteasome system. *Mol. Biol. Cell* **18,** 153–165 (2007).
23. Eisele, F. & Wolf, D. H. Degradation of misfolded protein in the cytoplasm is mediated by the ubiquitin ligase Ubr1. *FEBS Lett.* **582,** 4143–4146 (2008).
24. Heck, J. W., Cheung, S. K. & Hampton, R. Y. Cytoplasmic protein quality control degradation mediated by parallel actions of the E3 ubiquitin ligases Ubr1 and San1. *Proc. Natl Acad. Sci. USA* **107,** 1106–1111 (2010).
25. Nillegoda, N. B. *et al.* Ubr1 and Ubr2 function in a quality control pathway for degradation of unfolded cytosolic proteins. *Mol. Biol. Cell* **21,** 2102–2116 (2010).
26. Minami, R. *et al.* BAG-6 is essential for selective elimination of defective proteasomal substrates. *J. Cell Biol.* **190,** 637–650 (2010).
27. Ernst, R. *et al.* Enzymatic blockade of the ubiquitin–proteasome pathway. *PLoS Biol.* **8,** e1000605 (2011).
28. Wang, Q. *et al.* A chaperone holdase maintains polypeptides in soluble states for proteasome degradation. *Mol. Cell* doi:10.1016/j.molcel.2011.05.010 (in the press).
29. Garrison, J. L., Kunkel, E. J., Hegde, R. S. & Taunton, J. A substrate-specific inhibitor of protein translocation into the endoplasmic reticulum. *Nature* **436,** 285–289 (2005).
30. Sharma, A., Mariappan, M., Appathurai, S. & Hegde, R. S. *In vitro* dissection of protein translocation into the mammalian endoplasmic reticulum. *Methods Mol. Biol.* **619,** 339–363 (2010).

Supplementary Information is linked to the online version of the paper at www.nature.com/nature.

Acknowledgements We are grateful to E. Whiteman and X. Li for carrying out the initial experiments for parts of this project, S.W. Kang, S. Shao, and Z. Zhang for discussions, P. Sengupta, J. Magadán, and C. Ott for constructs, J. Taunton and J. Garrison for cotransin, S. Shao for comments on the manuscript, and Y. Ye for discussions and sharing results before publication. This work was supported by the Intramural Research Program of the National Institutes of Health (R.S.H.) and a postdoctoral fellowship from The Wenner-Gren Foundations (T.H.).

Author Contributions T.H. performed most of the experiments, with contributions from A.S. (ubiquitination assays in modified lysates), M.M. (defining the substrate specificity of BAG6), H.D.E. (characterizing the Fr-RRL system), E.G. (BAG6 crosslinking analysis) and R.S.H. (*in vivo* studies). R.S.H. conceived the project, guided the experiments and wrote the paper with input from all of the authors.

Author Information Reprints and permissions information is available at www.nature.com/reprints. The authors declare no competing financial interests. Readers are welcome to comment on the online version of this article at www.nature.com/nature. Correspondence and requests for materials should be addressed to R.S.H. (hegde.science@gmail.com).

METHODS

Plasmids and antibodies. The SP64 vector-based constructs encoding bovine preprolactin, PrP, ΔSS-PrP (lacking residues 2–22), ΔSSΔGPI-PrP (additionally lacking residues 232–254) and HA-tagged PrP (with the epitope inserted at codon 50) have been characterized previously[3,5,29–32]. Prl-PrP and NPY-PrP encode versions in which the N-terminal signal sequence (residues 1–22) of PrP was replaced[5] with that of either bovine preprolactin or human neuropeptide Y (NPY). N3a-PrP contains a mutated signal sequence (WL was replaced with DD at residues 7 and 8) that is translocation deficient[5]. The lysine-free version of PrP was provided by C. Ott and made by standard mutagenesis methods. Wild-type Sec61β (appended at the C terminus with an epitope recognized by the 3F4 antibody), Sec61β(3R), Sec61β–CFP and CFP–Sec61β have been described previously[4,20]. Sec61β–TR (referred to as TR-β in the text and figures) contains the TMD of the human transferrin receptor (IAVIVFFLIGFMIGYLGY) at codon 50 in the cytosolic domain of Sec61β[4]. This positions the TMD of TR outside the ribosomal tunnel when the Sec61β TMD is inside the tunnel[4]. RT-β contains an irrelevant hydrophilic sequence (YPKYPIMNPIKKKTITAI) at the same position[4]. GFP, SS/GPI–GFP (containing the N-terminal signal sequence of bovine preprolactin and the C-terminal GPI anchoring sequence of PrP), ManII–GFP (containing the N-terminal type II signal anchor domain of Golgi α-mannosidase II) and SiT–GFP (containing the type II signal anchor domain of sialyl transferase) have been described previously[32–34]. The plasmid encoding Vpu (a type-I-signal-anchored membrane protein from HIV-1) was obtained from J. Bonifacino and J. Magadán[35]. An expression plasmid for bovine rhodopsin has been characterized[29]. For translations of full-length products, the open reading frames were PCR amplified using a forward 5′ primer annealing to or encoding an SP6 or T7 promoter, and a reverse primer in the 3′ untranslated region at least 100 nucleotides beyond the stop codon. For RNCs, the reverse primer annealed in the coding region and lacked a stop codon. PrP and Vpu RNCs included the entire open reading frame except for the stop codon. The RNCs of β-CFP encoded 46 residues beyond the TMD such that this domain would fully emerge from the ribosome. Similarly, the RNCs of TR-β and RT-β encoded up to and including the TMD of Sec61β such that the TR and RT sequences emerge from the ribosome. Genetic constructs encoding BAG6–Flag and ΔUBL-BAG6–Flag (lacking residues 15–89 of BAG6)—both encoding human BAG6 containing a C-terminal Flag epitope—were subcloned into a mammalian expression vector by using standard methods. Expression vectors for human TRC35 and UBL4A containing C-terminal Flag tags were obtained from OriGene. Expression vectors for shRNAs directed against human BAG6 were from OriGene. The target sequences were TGACGGCT CTGCTGTGGATGTTCACATCA and CAGCTATGTCATGGTTGGAACCT TCAATC. The irrelevant sequence used as a control was GCACTACCAG AGCTAACTCAGATAGTACT. Antibodies specific for BAG6, TRC40, TRC35, UBL4A and Sec61β have been described previously[4,36]. Anti-SRP54 (BD Biosciences), anti-ubiquitin (BIOMOL), and 3F4 anti-PrP monoclonal antibodies (Signet) were purchased.

***In vitro* translation.** *In vitro* transcription and translation in RRL was carried out with minor modifications to published procedures[30]. The most notable change was the inclusion in most experiments of 10 μM His-tagged ubiquitin (Boston Biochem) to facilitate the subsequent isolation of ubiquitinated products. Preliminary experiments showed that, at this concentration, endogenous ubiquitin was more than 90% competed out, resulting in few or no untagged ubiquitinated products. Translation times, unless otherwise indicated, were 1 h at 32 °C. Shorter times for tail-anchored proteins (as used in our earlier studies) resulted in very little ubiquitination[4,20], presumably because saturation of TRC40 is required before substrates occupy the Bag6 complex[4]. To generate RNCs, the translation times were typically reduced to 30 min to minimize spontaneous release or hydrolysis of the tRNA. Translocation assays into rough microsomes[5], inhibition by cotransin[29] and inactivation with NEM[37] treatment were carried out as previously described. For direct analysis or downstream immunoprecipitation, translation reactions were stopped, and the proteins were denatured using 1% SDS and heating to 100 °C. For other applications requiring native complexes (for example, crosslinking, affinity purification or downstream assays), samples were placed on ice, and subsequent manipulations were performed at 0–4 °C.

Sucrose gradient separation and crosslinking. To generate RNCs, translation reactions (typically 200 μl volume) were chilled on ice and immediately layered onto 2-ml 10–50% sucrose gradients in physiological salt buffer (PSB; 100 mM potassium acetate, 50 mM HEPES, pH 7.4, and 2 mM magnesium acetate). Centrifugation was carried out for 1 h at 55,000 r.p.m. at 4 °C in a TLS-55 rotor (Beckman), after which 200 μl fractions were removed from the top. The peak ribosomal fractions (6 and 7) were pooled and used as the RNCs. These were used immediately or flash frozen in liquid nitrogen for later use in RNC crosslinking or ubiquitination experiments. Chemical crosslinking experiments were essentially carried out as described previously[4,20]. Chilled translation reactions were layered onto 2-ml 5–25% sucrose gradients in PSB and centrifuged for 5 h at 55,000 r.p.m. at 4 °C in a TLS-55 rotor, after which 200 μl fractions were removed from the top. Crosslinking experiments used 250 μM BMH, except for in experiments to detect SRP interaction, which used 200 μM DSS. Reactions were carried out for 30 min at either 0 °C (BMH) or 25 °C (DSS) and quenched with 25 mM 2-mercaptoethanol (BMH) or 100 mM Tris (DSS). The samples were subsequently denatured and subjected to direct analysis or immunoprecipitation as described below. Photocrosslinking was carried out by following published methods[38], except that we used the Fr-RRL system for translation and benzophenone-modified lysyl-tRNA (tRNA Probes). The absence of endogenous charged tRNAs and haemoglobin increased photocrosslinker incorporation and photolysis, respectively. Photolysis was carried out for 15 min on ice, and the samples were analysed directly.

Modified translation extracts. Fr-RRL was typically prepared from 25 ml RRL (Green Hectares) that had first been treated with haemin and micrococcal nuclease. Its characterization will be described in a future publication, but its preparation is as follows. All procedures were carried out on ice or at 4 °C. The lysate was centrifuged at 100,000 r.p.m. for 40 min in a TLA100.4 rotor (Beckman). The supernatants were pooled, and the tubes rinsed (without disrupting the ribosomal pellet) with an equal volume of column buffer (20 mM Tris, pH 7.5, 20 mM KCl, 0.1 mM EDTA and 10% glycerol), which was added to the supernatant. The pellet was resuspended by dounce homogenization in ribosome wash buffer (RWB; 20 mM HEPES, pH 7.5, 100 mM potassium acetate, 1.5 mM magnesium acetate and 0.1 mM EDTA), layered onto a 1 M sucrose cushion in RWB, and re-isolated by centrifugation at 100,000 r.p.m. for 1 h in a TLA100.4 rotor. The final pellet was resuspended in one-tenth of the original lysate volume and defined as 'native ribosomes'. The ribosome-free supernatant from above was applied to a 10 ml DEAE column at a flow rate of ~1 ml min^{-1} and washed with column buffer until the red haemoglobin was removed (~50 ml). The elution was carried out in a single step with 50 ml column buffer containing 300 mM KCl. The eluate was adjusted slowly with solid ammonium sulphate to 75% saturation (at 4 °C) with constant stirring. After 1 h mixing, the precipitate was recovered by centrifugation at 15,000 r.p.m. in a JA-17 rotor (Beckman). The supernatant was discarded, and the pellet was dissolved in a minimal volume (~8 ml) of dialysis buffer (20 mM HEPES, pH 7.4, 100 mM potassium acetate, 1.5 mM magnesium acetate, 10% glycerol and 1 mM DTT). This solution was dialysed against two changes of dialysis buffer overnight, recovered, adjusted to 10–12 ml (that is, twice the original concentration) and flash frozen in liquid nitrogen. To make a translation-competent Fr-RRL, the native ribosomes and dialysed DEAE eluate were adjusted to 72 mM potassium acetate, 2.5 mM magnesium acetate, 10 mM HEPES, pH 7.4, 2 mM DTT, 0.2 mg ml^{-1} liver tRNA, 1 mM ATP, 1 mM GTP, 12 mM creatine phosphate, 40 μg ml^{-1} creatine kinase, 40 μM each amino acid (except for methionine) and 1 μCi $μl^{-1}$ [^{35}S]methionine. The concentration of ribosomes and lysate was the same as that for RRL. Immunodepletions of RRL were carried out as described previously[4].

Ubiquitination assays. The human E1 enzyme and all mammalian E2 enzymes were obtained from Boston Biochem. For full-length proteins, translations containing 10 μM His–ubiquitin were carried out for 1 h at 32 °C. In Fr-RRL, post-translational ubiquitination was initiated by adding E2 enzyme to a final concentration of 250 nM and further incubating for 1 h. For RNCs, samples were supplemented (as indicated in the figures) with E1 enzyme (85 nM), E2 enzyme (usually 250 or 500 nM), cytosol (RRL or Fr-RRL, at the same concentration as in the translations), 10 μM His–ubiquitin, an ATP-regenerating system (1 mM ATP, 10 mM creatine phosphate and 40 μg ml^{-1} creatine kinase) and 1 mM puromycin. Reaction conditions were 100 mM potassium acetate, 50 mM HEPES, pH 7.4, 5 mM $MgCl_2$ and 1 mM DTT. Incubation was for 1 h at 32 °C. On-bead ubiquitination of affinity-purified products was carried out under the same conditions, except for without puromycin. To prepare the affinity-purified substrate, translation reactions in Fr-RRL were chilled on ice, diluted to 1 ml in PSB and incubated with immobilized antibodies against the HA epitope (for PrP–HA and Vpu–HA) or Sec61β. In Supplementary Fig. 9, the translation reactions were supplemented with Flag-tagged BAG6 or ΔUBL-BAG6 (each added to twofold excess above endogenous BAG6 levels), and anti-Flag beads (Sigma) were used for the pull-down. After 1 h, the resin was washed five times in PSB, and the residual buffer was carefully removed before adding the ubiquitination components as above. The reaction was incubated with constant low-level shaking (in a Thermomixer, Eppendorf) at 32 °C for 1 h. SDS (1%) was added directly to the reactions, which were analysed directly and after ubiquitin pull-downs.

Cell culture studies. Culture, transfection and immunoblotting analysis of N2a cells (dominant-negative inhibition experiments) and HeLa cells (for shRNA experiments) were carried out as described previously[2,3]. Cells were seeded in 24-well dishes the day before transfection. For the dominant-negative experiments, the plasmids were mixed in the ratios indicated in Supplementary Fig. 20 and transfected using Lipofectamine 2000 (Invitrogen) according to the manufacturer's instructions. At 24 h after transfection, the cells were harvested in 1% SDS;

the DNA was sheared by vortexing and boiling; and the total sample was analysed by SDS–PAGE and immunoblotting. For shRNA experiments, each well received a mixture of 550 ng shRNA plasmid, 200 ng PrP expression plasmid and 50 ng CFP expression plasmid. Transfection was effected with Lipofectamine 2000. Examination of CFP fluorescence verified at least 50% transfection efficiency. The cells were cultured for ~100 h before collection and analysis by immunoblotting.

BAG6 purification. Full-length BAG6 or ΔUBL-BAG6 tagged at the C terminus with a Flag epitope was overexpressed by transient transfection of HEK-293T cells. *Trans*IT reagent (Mirus) was used. After 3 days of expression, the cells were collected in 50 mM HEPES, pH 7.4, 150 mM potassium acetate, 5 mM magnesium acetate and 1% deoxy Big CHAP. The soluble extract was incubated with immobilized anti-Flag antibodies (Sigma) with constant mixing, and the resin was washed four times with high salt lysis buffer containing 400 mM potassium acetate and then twice with detergent-free lysis buffer containing 230 mM potassium acetate. Elution was carried out with 1 mg ml^{-1} competing peptide at room temperature. The final protein was checked by using colloidal Coomassie blue (Supplementary Fig. 16), and its concentration relative to that in RRL was determined by immunoblotting of serial dilutions. Blotting also confirmed the lack of TRC35 and UBL4A in BAG6 prepared by this method.

Miscellaneous biochemistry. Immunoprecipitation assays were carried out as described previously[5,36]. Pull-down assays with Co^{2+} immobilized on chelating sepharose were performed on samples denatured in boiling 1% SDS and then diluted tenfold in cold (4 °C)0.5% Triton X-100, 25 mM HEPES, 100 mM NaCl and 10 mM imidazole. The complete denaturation step is essential for samples containing RRL because the haemoglobin is a strong Co^{2+}-binding protein in its native state. Typically, 10 µl packed resin was used per sample, and after incubation for 1–2 h at 4 °C, the resin was washed three times in the above buffer and eluted in SDS–PAGE sample buffer containing 20 mM EDTA. SDS–PAGE was carried out using 8.5% or 12% tricine gels. Figures were prepared using the programs Photoshop and Illustrator (Adobe).

31. Emerman, A. B., Zhang, Z. R., Chakrabarti, O. & Hegde, R. S. Compartment-restricted biotinylation reveals novel features of prion protein metabolism *in vivo*. *Mol. Biol. Cell* **21,** 4325–4337 (2010).
32. Ashok, A. & Hegde, R. S. Retrotranslocation of prion proteins from the endoplasmic reticulum by preventing GPI signal transamidation. *Mol. Biol. Cell* **19,** 3463–3476 (2008).
33. Cole, N. B. *et al.* Diffusional mobility of Golgi proteins in membranes of living cells. *Science* **273,** 797–801 (1996).
34. Wu, M. M. *et al.* Organelle pH studies using targeted avidin and fluorescein–biotin. *Chem. Biol.* **7,** 197–209 (2000).
35. Magadán, J. G. *et al.* Multilayered mechanism of CD4 downregulation by HIV-1 Vpu involving distinct ER retention and ERAD targeting steps. *PLoS Pathogens* **6,** e1000869 (2010).
36. Fons, R. D., Bogert, B. A. & Hegde, R. S. Substrate-specific function of the translocon-associated protein complex during translocation across the ER membrane. *J. Cell Biol.* **160,** 529–539 (2003).
37. Gilmore, R., Blobel, G. & Walter, P. Protein translocation across the endoplasmic reticulum. I. Detection in the microsomal membrane of a receptor for the signal recognition particle. *J. Cell Biol.* **95,** 463–469 (1982).
38. Krieg, U. C., Walter, P. & Johnson, A. E. Photocrosslinking of the signal sequence of nascent preprolactin to the 54-kilodalton polypeptide of the signal recognition particle. *Proc. Natl Acad. Sci. USA* **83,** 8604–8608 (1986).

doi:10.1038/nature10181

I. Technical notes relating to each of the main figures.

Notes for Fig. 1.

Panel a – Translation time was 1 h at 32°C. The translated products are detected by autoradiography via the ^{35}S-Methionine incorporated into the newly synthesized protein. Ubiquitinated products are not degraded in this system due to the presence of Hemin in the lysate. Hemin inhibits both p97 activity and proteaseome activity. De-ubiquitination activity in the lysate is relatively modest, as only a small increase in ubiquitination was observed in the presence of Ubiquitin-aldehyde. His-Ubiquitin was included in the translation reactions at 10 uM. The ubiquitinated products (right panel) were isolated by immobilized Co^{+2} after complete denaturation of the translation reaction, and detected by autoradiography. Note that the N-terminus of PrP contains a copper-binding domain, contributing to a small amount of background in the Co^{+2} pulldowns in this and other experiments (i.e., some non-ubiquitinated product is also recovered).

Panel b – Time course of an experiment as in panel A without microsomes. The top panel shows an autoradiograph of ubiquitinated PrP, isolated via the His-Ubiquitin. The bottom panel shows full length PrP detected by autoradiography of total translation products. Note that ubiquitination occurs very shortly after synthesis. This is different than a tail-anchored protein destined for post-translational insertion into the ER, where ubiquitination lags behind synthesis by ~10-20 min (see Sup. Fig. S23).

Panel c – In vitro synthesized transcripts were generated of the complete PrP coding region (residues 1-254). The 'terminated' transcript contains a stop codon plus ~200 nucleotides of a 3'UTR, while the 'truncated' transcript ends precisely at the last codon (and therefore does not contain an in-frame stop codon). This results in a peptidyl-tRNA that remains tethered to the ribosome at the P-site, and is generally stable for the ~1 h time-frame of the experiment. Analysis of the truncated product on SDS-PAGE shows some tRNA-associated product, which is partially hydrolyzed during sample preparation and electrophoresis under the slightly basic conditions. The identity of the band (arrowhead) as tRNA-associated was verified by RNAse digestion just before electrophoresis. The ribosome-nascent chains of truncated PrP were isolated by sucrose gradient centrifugation (to remove bulk cytosol) and treated with 1 mM puromycin for 1 h to release the chains. The release reactions contained an energy regenerating system, His-Ubiquitin, E1 enzyme, and E2 enzyme. One reaction also contained RRL (cytosol), while the other contained a matched buffer. Note that cytosol is needed to get ubiquitination of substrate.

Panel d – Both the signal sequence and GPI anchoring sequence are hydrophobic, and both contribute to the overall ubiquitination efficiency of PrP. The precise sequence of the signal was not important since different signal sequences of varying amino acid composition and sequence facilitated ubiquitination when used to replace the PrP signal sequence.

Notes for Fig. 2.

Panel a – The Fr-RRL system is essentially a translation-competent reaction corresponding to the classic 'Fraction II' from the original ubiquitination studies of Hershko, Ciechanover, and Rose.

This fraction does not contain much ubiquitin, hence requiring supplementation. Ubiquitin supplementation however is not enough to complement ubiquitination of MLPs, even though ubiquitination of other proteins is restored (see Sup. Fig. S7). This is because in addition to ubiquitin, subsets of E2s and E3s are also missing from the reaction.

Panel b – Translation time was for 1 h at 32°C in the Fr-RRL system without or with 250 nM UbcH5a. All reactions contained 10 uM His-Ubiquitin. For post-translational ubiquitination, UbcH5a was added after the translation, and incubated for another hour at 32°C. Ubiquitinated products were isolated by immobilized Co^{+2}, while total products were analyzed directly, and detected by autoradiography. The fact that UbcH5a can be added after translation means that the PrP substrate is being maintained in a ubiquitination-competent state after its synthesis, and that it does not need to be ubiquitinated immediately.

Panel c - For immunoaffinity purification, the PrP construct was appended with an HA epitope, inserted at residue 50 in the flexible N-terminal domain. After translation, PrP-HA was purified under native, non-detergent conditions, using immobilized anti-HA antibodies. The absence of detergent is important because the hydrophobic interaction between PrP and Bag6 is sensitive to detergent (but relatively insensitive to salt). The beads were washed in detergent-free buffer and the ubiquitination reaction performed directly on the beads. Ubiquitination was for 1 h at 32°C. After the reaction, the samples were completely denatured and the ubiquitinated products isolated via immobilized Co^{+2}. The fact that cytosol is not needed suggests that the PrP pulldowns contain an active E3 enzyme.

Panel d – PrP-HA was used for this experiment to facilitate the ubiquitination assays. Chemical crosslinking was with BMH at 250 uM on ice for 30 min. Similar results were seen with DSS crosslinking, but typically generated more background. For the ubiquitination assays, each fraction was affinity purified via the HA tag as in panel c and subjected to ubiquitination on the beads. The relative ubiquitination was quantified and graphed.

Panel e – After translation of the indicated constructs, the samples were separated on a sucrose gradient as in panel d, and fractions 6-10 were pooled for the crosslinking reactions.

Notes for Fig. 3.

Panel a – The extra TMD inserted into Sec61β was from Transferrin Receptor (TR), which has been showed experimentally to interact with SRP as a nascent chain. The control hydrophilic sequence is the random sequence encoded by the same oligos inserted in the reverse orientation. The mutation within the TMD of Sec61β introduces three Arginines, and this has been shown to disrupt binding to the TA insertion machinery, including Bag6 and TRC40.

Panels b and c – Crosslinking was with DSS at 200 uM for 30 min at 25°. The same results were obtained with BMH crosslinking for the Bag6 interaction, but BMH does not effectively crosslink SRP, presumably because of a lack of suitably positioned cysteine residues.

Panel d – All proteins were full length (i.e., not to be confused with the RNCs in panels b and c). Affinity purification was performed via anti-Sec61β antibodies under detergent-free conditions

to preserve the hydrophobic interactions between substrates and Bag6 and/or TRC40.

Notes for Fig. 4.

Panel a – Translation times were for 1 h at 32°C. Reactions contained 10 uM His-Ubiquitin to allow purification of the ubiquitinated products. Immunodepletion was via an anti-Bag6 antibody column, and the non-depleted control used an anti-GFP antibody column. Depletion efficiency was judged by immunoblotting to be ~90%. Depletion of Bag6 results in at least 80% co-depletion of its associated factors Ubl4A and TRC35.

Panel b – The purified Bag6 and ΔUbl-Bag6 did not contain its associated factors Ubl4A and TRC35, while the native Bag6 complex did. Relative levels were assessed by immunoblotting of serial dilutions.

Panel c – Crosslinking reactions were performed as in Figure 2e. The top panel shows high molecular weight crosslinking products. The identity of the band as a Bag6 crosslink was verified by both anti-Bag6 and anti-FLAG IPs. As expected, the recombinant Bag6 and ΔUbl-Bag6 were immunoprecipitated with anti-FLAG and anti-Bag6, while the endogenous Bag6 was only immunoprecipitated with anti-Bag6.

Panels d and e – Cells were harvested ~22-24 h after transfection. The increase in N3a-PrP levels seen with ΔUbl-Bag6 or with proteasome inhibitor is due to decreased degradation, and not increased synthesis since control proteins (e.g., GFP) were verified to be unaffected in their levels under identical conditions. Similarly, the matched construct lacking hydrophobic elements (ΔSSΔGPI-PrP) was also unaffected in its levels by ΔUbl-Bag6, illustrating that ΔUbl-Bag6 does not affect protein production.

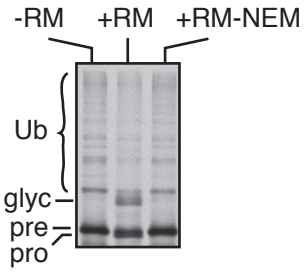

Sup. Fig. S1. PrP that fails targeting is ubiquitinated in vitro. PrP was translated for 1 hour in reticulocyte lysate lacking or containing mock-treated or NEM-treated ER-derived rough microsomes (RMs). Treatment of RMs was with 0 or 3 mM N-ethyl maleimide (NEM) for 15 min at 25°C. DTT was then added to 10 mM to inactivate NEM, and the microsomes were re-isolated by centrifugation prior to use in the assay. Note that these manipulations lead to a slight loss of targeting activity of the control RMs, while NEM-treated RMs are completely inactive due to alkylation of the SRP-receptor. The PrP that fails targeting to the NEM-inactivated RMs is ubiquitinated.

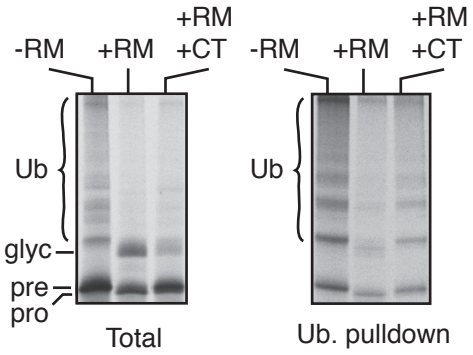

Sup. Fig. S2. PrP that fails translocation is ubiquitinated. PrP was translated in reticulocyte lysate lacking or containing ER-derived rough microsomes (RMs), without or with the translocation inhibitor cotransin (CT, added to 10 uM; Garrison et al., 2005, Nature, 436:285-9). Translation reactions contained 10 uM His-ubiquitin. After translation, an aliquot was analyzed directly (left panel; 'Total'), while the remainder was pulled down with immobilized Co^{+2} to recover ubiquitinated products (right panel; 'Ub pulldown'). Note that PrP is only ~50% inhibited in its translocation by cotransin. The positions of precursor, processed, glycosylated, and ubiquitinated forms of PrP are indicated. Translation time was 1 h.

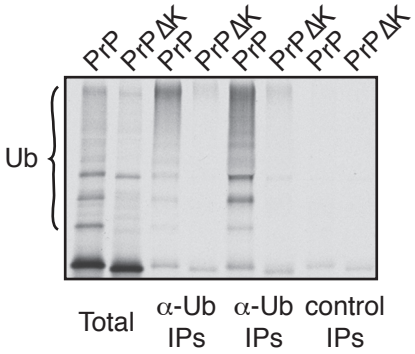

Sup. Fig. S3. Lysines in PrP are needed for ubiquitination. PrP and a construct with all Lysines mutated to Arginines (PrPΔ K) were translated in reticulocyte lysate for 1 h. An aliquot was analyzed directly ('Total'), while the remainder was immunoprecipitated with two different anti-Ubiquitin antibodies or an unrelated control antibody. Re-introduction of a single Lysine into PrP was sufficient to restore ubiquitination (unpublished observations).

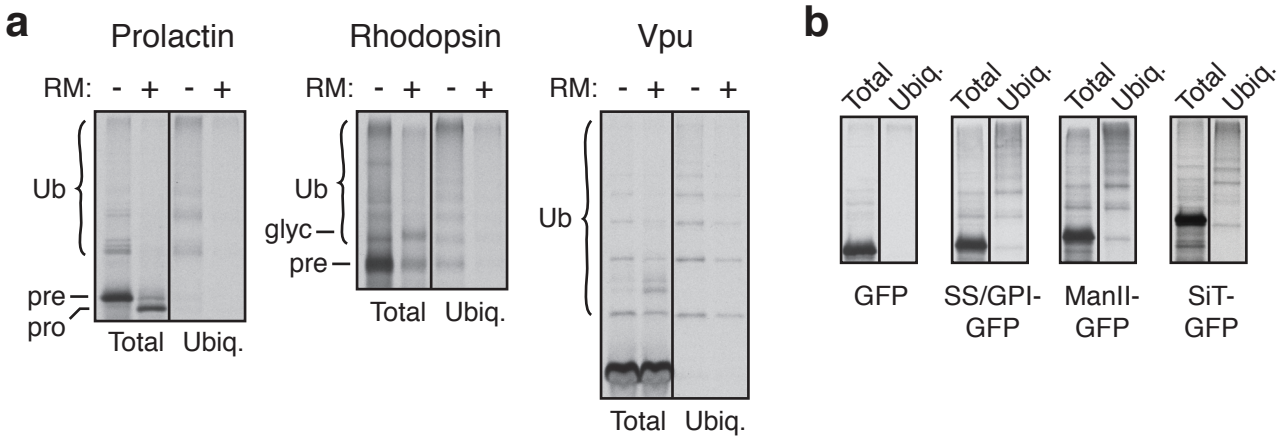

Sup. Fig. S4. Analysis of various proteins for ubiquitination in vitro. (a) The indicated proteins were translated in reticulocyte lysate (supplemented with 10 uM His-ubiquitin) without or with RM. An aliquot was analyzed directly ('Total'), while the remainder was pulled down with immobilized Co^{+2} to enrich for ubiquitinated species ('Ubiq.'). Prolactin is a secretory protein with an especially hydrophobic signal sequence; Rhodopsin is a 7-TM domain protein; Vpu is type I signal anchored membrane protein (from HIV). (b) The indicated proteins were translated in reticulocyte lysate supplemented with 10 uM His-ubiquitin. An aliquot was analyzed directly ('Total'), while the remainder was pulled down with immobilized Co^{+2} to enrich for ubiquitinated species ('Ubiq.'). SS/GPI-GFP contains the N-terminal signal sequence from Prolactin and C-terminal GPI anchoring signal from PrP; SiT-GFP and ManII-GFP contains the Type I signal anchor sequences from Sialyl transferase and Golgi Mannosidase II, respectively, at the N-terminus. Note that GFP is poorly ubiquitinated, but becomes a much better target when appended with targeting/translocation signals.

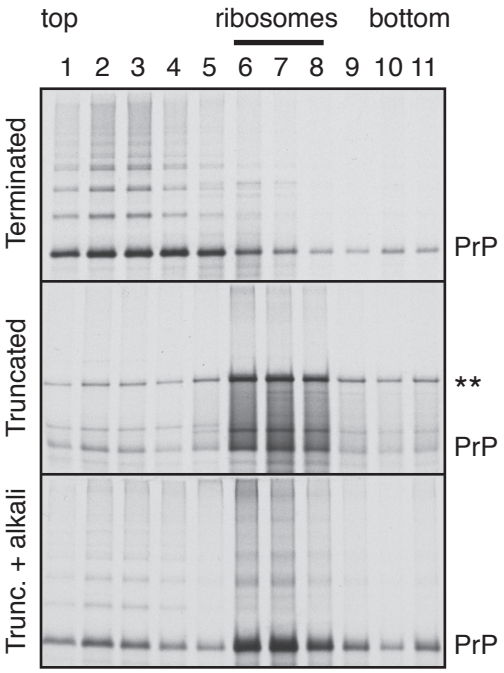

Sup. Fig. S5. PrP is ubiquitinated after ribosomal release. PrP transcript containing (terminated) or lacking (truncated) a stop codon was translated in reticulocyte lysate, separated on a 10-50% sucrose gradient, and each of 11 fractions analyzed by SDS-PAGE. The samples in the bottom gel were adjusted to pH 11 before electrophoresis to hydrolyze tRNA, while the samples in the middle gel were maintained under near-neutral conditions to preserve the peptidyl-tRNA species (indicated with asterisks). The position of ribosomes in the gradient is indicated.

Note that little or no ubiquitination is seen in the ribosomal fraction of truncated PrP nascent chains. The only ubiquitination observed in the truncated sample appears to arise from spontaneously released polypeptides. The smear seen in the ribosomal fractions is not likely to be ubiquitination since it could not be recovered by anti-ubiquitin antibodies (not shown), and may instead represent some PrP aggregation.

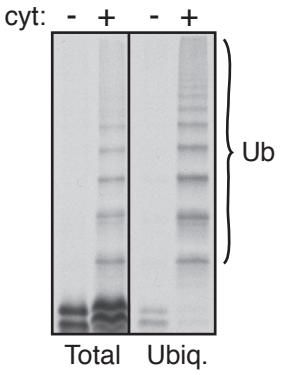

Sup. Fig. S6. Vpu becomes ubiquitinated upon release into the cytosol. Ribosome-nascent chains encoding Vpu (an 81-residue polypeptide, with the first ~20 residues encoding a TM domain) were isolated from a sucrose gradient (e.g., as in Sup. Fig. S5) and released with puromycin in the presence of an energy regenerating system, E1 (100 nM), UbcH5 (250 nM), and His-ubiquitin (10 uM), without or with cytosol ('cyt.'). After incubation for 60 min, the samples were either analyzed directly ('Total') or after pulling down ubiquitinated products with immobilized Co^{+2} ('Ubiq'). The experiment in Fig. 1c was performed exactly the same way.

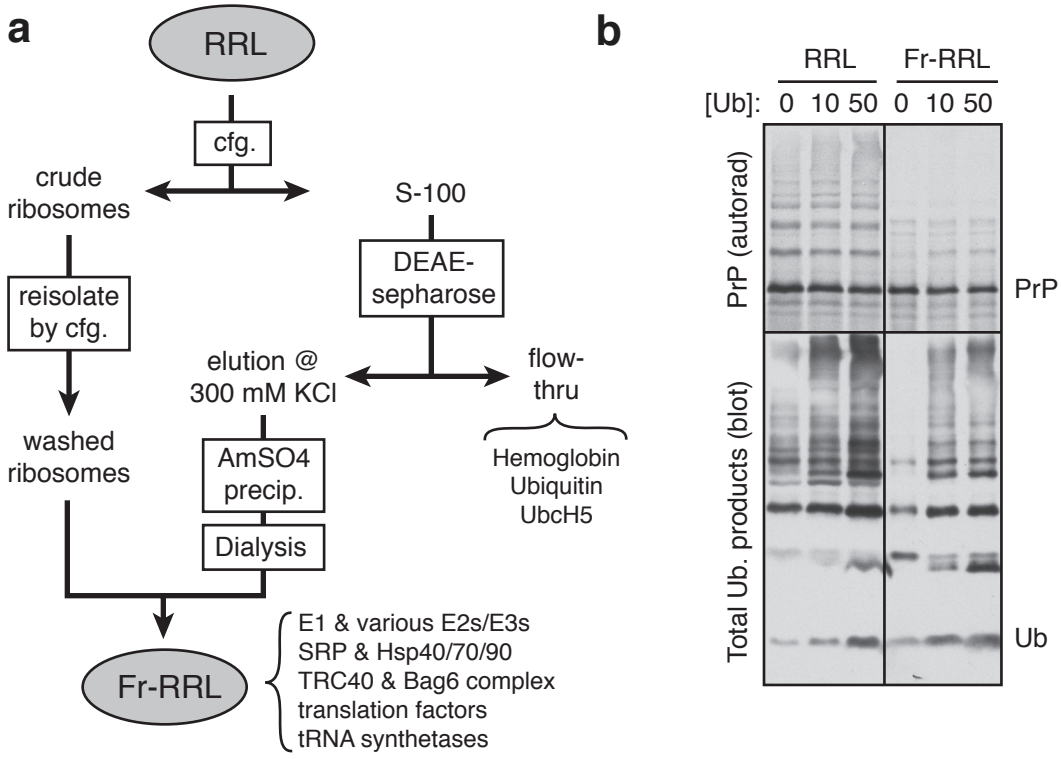

Sup. Fig. S7. A fractionated translation system from RRL. (a) Schematic diagram of the fractionation procedure to produce Fr-RRL. Ribosomes are removed from RRL by centrifugation, washed, and added back to a DEAE-elution fraction. This system, when complemented with tRNAs, amino acids, and an energy regenerating system, is competent for translation. Indicated is a partial list of key factors verified (by blots and/or activity) to be in Fr-RRL, and those known to be lost in the DEAE flow thru fraction. (b) PrP was translated in either RRL or Fr-RRL supplemented with the indicated concentrations (in uM) of His-ubiquitin. The translation products were separated by SDS-PAGE, transferred to nitrocellulose, and visualized by autoradiography to detect the translated PrP (top panel; the image is the same as that in Fig. 2a). This same blot was also probed with anti-ubiquitin to detect endogenous ubiquitinated species (bottom panel). This illustrates that the Fr-RRL system, when supplemented with ubiquitin, is competent for ubiquitination of various endogenous proteins, but is substantially impaired for ubiquitination of non-translocated PrP.

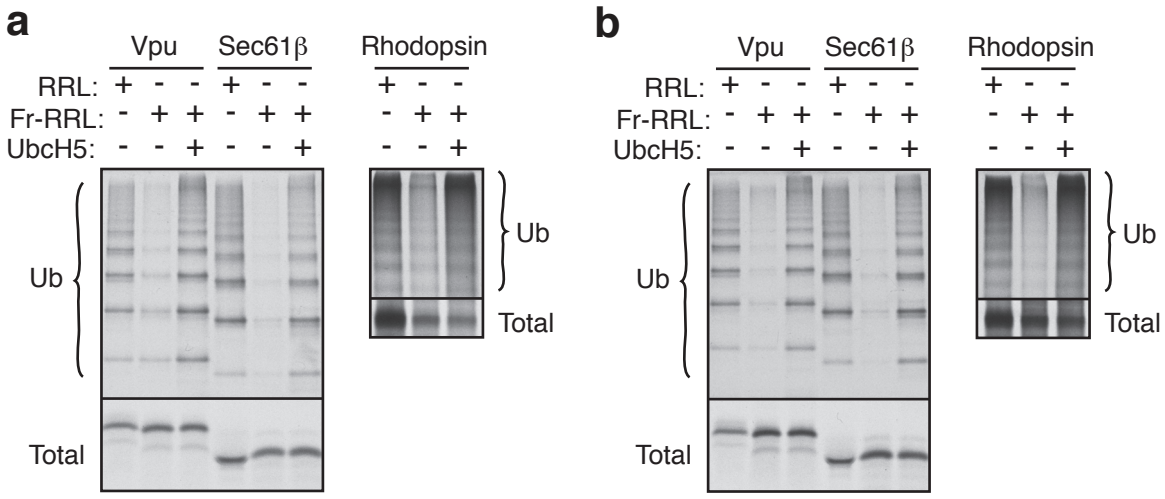

Sup. Fig. S8. Various MLPs require UbcH5 for ubiquitination in vitro. Ubiquitination assays for various MLPs were performed in RRL and Fr-RRL similarly to Fig. 2a and 2b. The indicated constructs were translated in either RRL or Fr-RRL supplemented with 10 uM His-ubiquitin. Where indicated, 250 nM UbcH5 (isoform a) was included co-translationally (panel a) or added after translation (panel b). In the co-translational reactions, total translation time was 1 h. In the post-translational reaction, translation was also for 1 h, but the incubation continued for an additional 1 h after UbcH5 was added. The samples were either analyzed directly ('Total') or after pulling down ubiquitinated products with immobilized Co^{+2} (top panels). Note that some proteins (e.g., Rhodopsin) do not translate as well in Fr-RRL as in RRL for unclear reasons. Nonetheless, it is apparent that upon replenishment of Fr-RRL with UbcH5 (either co- or post-translationally), levels of ubiquitination are comparable to RRL, suggesting that this was the main if not only factor missing in Fr-RRL needed for this pathway.

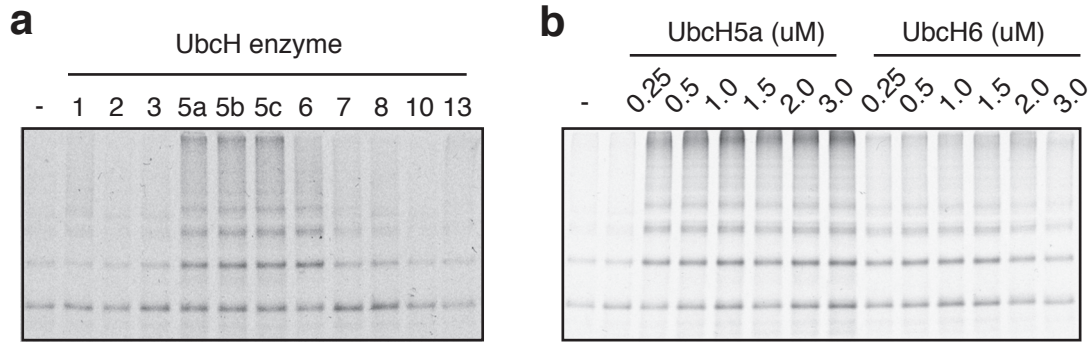

Sup. Fig. S9. Analysis of various E2 enzymes for ability to restore ubiquitination activity to Fr-RRL. (a) Ribosome-nascent chains of PrP were released with puromycin into Fr-RRL supplemented with 10 uM His-ubiquitin, 100 nM E1 enzyme, and an ATP regenerating system. The indicated E2 enzyme was included at 3 uM. After 1 h at 32°C, the ubiquitinated products were captured with immobilized Co^{+2} and analyzed by SDS-PAGE. UbcH5 isoforms and highly related UbcH6 enzyme have significant activity, while the others are less active. (b) An experiment as in panel a comparing UbcH5a to UbcH6 at various concentrations. Note that UbcH5a is highly active even at the lowest concentration (250 nM), while UbcH6 was substantially less active at all concentrations. Furthermore, immunoblotting of fractions during the Fr-RRL preparation confirmed that UbcH5 was lost during the ion exchange step and therefore not present in the final Fr-RRL sample.

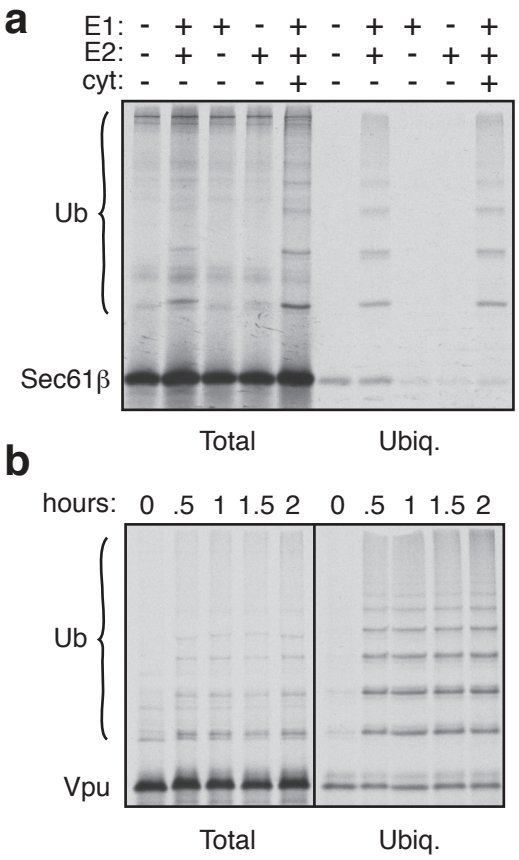

Sup. Fig. S10. Ubiquitination of affinity purified Sec61β and Vpu with purified components. (a) Sec61β was translated in Fr-RRL and immunoaffinity purified under non-denaturing, non-detergent conditions using an anti-Sec61β antibody resin. After washing of the resin, the indicated components were added: 100 nM E1, 250 nM UbcH5, or cytosol. All reactions contained 10 uM His-ubiquitin and an ATP-regenerating system (1 mM ATP, 10 mM Creatine phosphate, 40 ug/ml Creatine Kinase). After incubation for 1 h at 32°C, the samples were either analyzed directly ('Total') or after pulling down ubiquitinated products with immobilized Co^{+2} ('Ubiq'). The experiment in Fig. 2c was performed exactly the same way. (b) HA-tagged Vpu was translated in Fr-RRL. Anti-HA antibodies were added, and after 30 min on ice, the antibody complexes were recovered under non-denaturing, non-detergent conditions using immobilized Protein A. The washed beads were then supplemented with 100 nM E1, 250 nM UbcH5, 10 uM His-ubiquitin and an ATP-regenerating system, and incubated for the indicated times at 32°C. The samples were either analyzed directly ('Total') or after pulling down ubiquitinated products with immobilized Co^{+2} ('Ubiq'). Note that not every protein incubated as above gets ubiquitinated, since a Sec61β construct lacking its TMD was not ubiquitinated (data not shown), and sub-populations of Vpu or PrP are not ubiquitinated under these same conditions (e.g., Fig. 2d and Sup. Fig. S11).

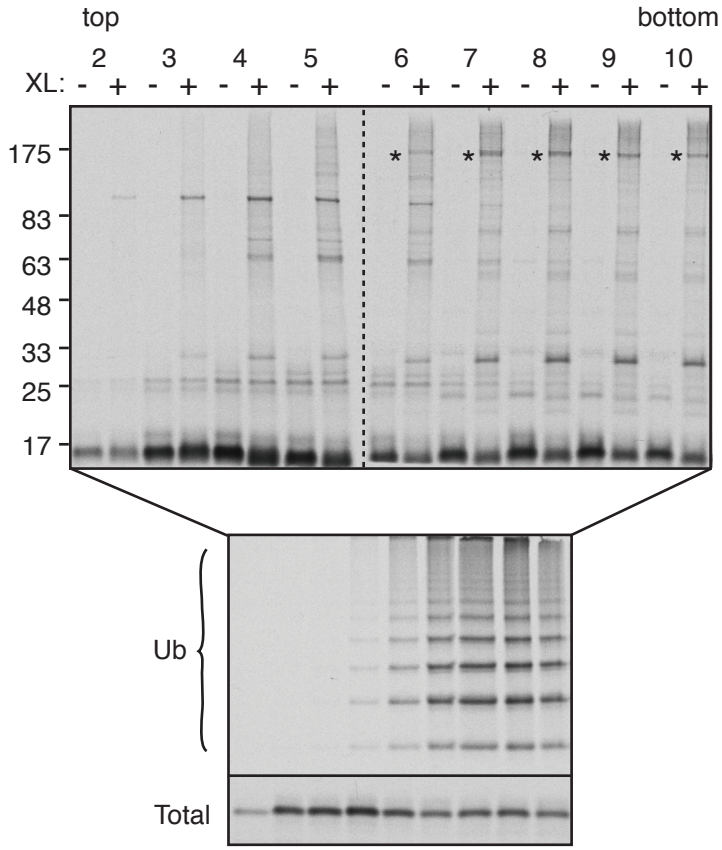

Sup. Fig. S11. Correlation of p150 crosslinking with ubiquitination of Vpu. Vpu-HA was translated in Fr-RRL and separated into 10 fractions on a 5-25% sucrose gradient. Each fraction was subjected to chemical crosslinking with 250 uM bis-maleimido-hexane (BMH), a sulfhydryl-reactive crosslinker, and analyzed by SDS-PAGE (top gel). The position of a ~150 kD crosslinking partner is indicated with an asterisk. In parallel, Vpu-HA from each fraction was affinity purified with immobilized anti-HA and assayed for ubiquitination competence by addition of E1, E2, His-ubiquitin, and energy (as in Sup. Fig. S10 above). An aliquot of the total recovered material ('Total') and ubiquitinated products (captured via the His-ubiquitin) is shown. Note that ubiquitination activity correlates with the p150 crosslink. Note also that Vpu recovered from some fractions (e.g., 2-5) is not ubiquitinated effectively, illustrating that the E1 and E2 enzymes are not by themselves sufficient to ubiquitinate Vpu.

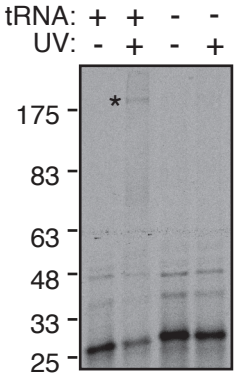

Sup. Fig. S12. Photo-crosslinking of PrP to p150. PrP was translated in Fr-RRL containing or lacking a benzophenone-modified Lysyl-tRNA. The translation products were then irradiated with UV light to induce photo-crosslinking, and analyzed by SDS-PAGE. The asterisk indicates the position of a ~150 kD crosslinking product.

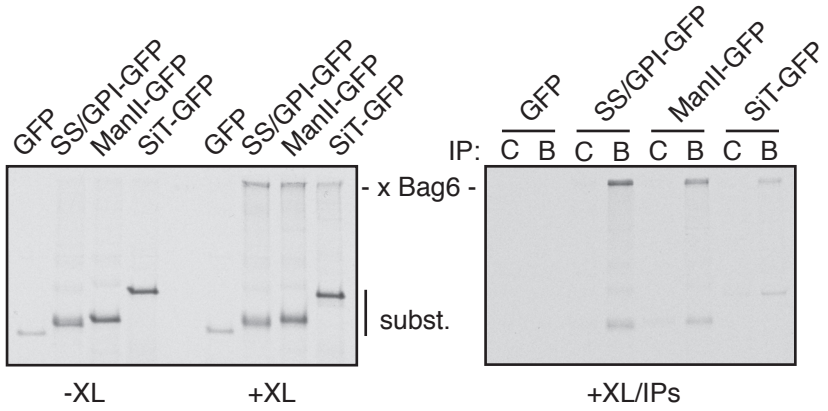

Sup. Fig. S13. Bag6 interacts with hydrophobic domains. GFP or versions appended with the indicated hydrophobic domains were translated in vitro, separated by a 5-25% sucrose gradient as in Fig. 2d, and the pooled fractions 6-10 subjected to chemical crosslinking with BMH. The samples before and after crosslinking are shown in the left panel. The right panel shows the crosslinking products immunoprecipitated with either control (C) or Bag6 (B) antibodies. 'SS/GPI' refers to the signal sequence and GPI anchoring sequence from Prolactin and PrP, respectively. 'ManII' refers to the TMD of Golgi Mannosidase II. 'SiT' refers to the cytosolic and TMD regions of Golgi Sialyl-transferase.Note that modifying GFP with hydrophobic targeting elements results in Bag6 interaction.

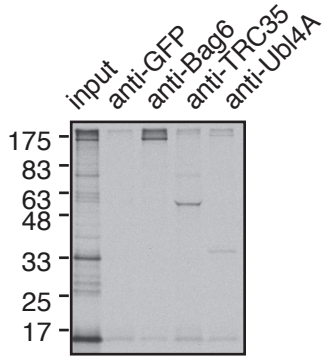

Sup. Fig. S14. Vpu crosslinking to the Bag6 complex. Vpu was translated in Fr-RRL, separated on a 5-25% sucrose gradient (as in Sup. Fig. S11), and fractions 6-10 pooled. The pooled sample was treated with BMH crosslinker on ice for 30 min, and either analyzed directly ('input') or subjected to immunoprecipitation with the indicated antibodies. As observed before (Mariappan et al., 2010, Nature, 466:1120-4), Ubl4A crosslinks only weakly to substrate, probably because it does not make direct contact with substrate but is in the vicinity due to its being part of the Bag6 complex. Affinity purification of HA-tagged Vpu (without cross-linking, under native conditions) confirmed its co-precipitation with all three subunits of the Bag6 complex by immunoblotting (not shown).

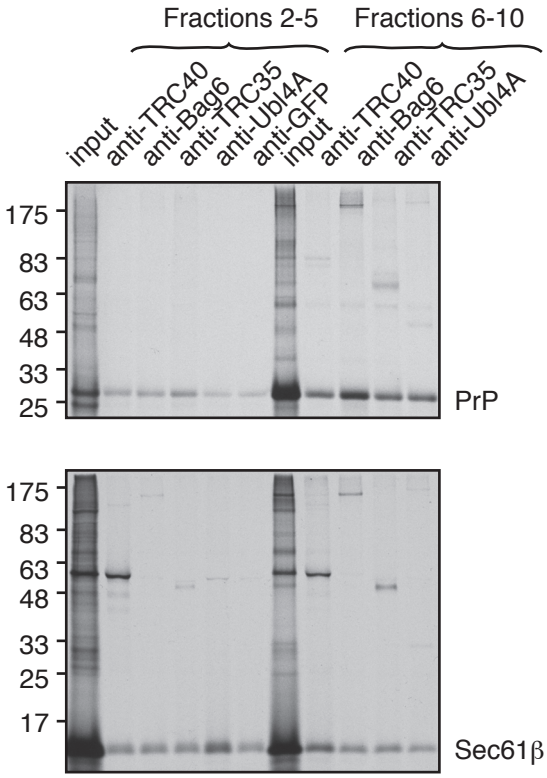

Sup. Fig. S15. PrP and Sec61β crosslinking to the Bag6 complex. PrP and Sec61β were translated in Fr-RRL, separated on a 5-25% sucrose gradient (as in Sup. Fig. S11), and fractions 2-5 and 6-10 were pooled. The pooled samples were treated with BMH crosslinker on ice for 30 min, and either analyzed directly ('input') or subjected to immunoprecipitation with the indicated antibodies. Note that both PrP and Sec61β crosslink to all three components of the Bag6 complex (Ubl4A only weakly). However, the major crosslink for Sec61β was TRC40, as observed before (Stefanovic and Hegde, 2007, Cell, 128:1147-59), consistent with the fact that Sec61β bound to the Bag6 complex is transferred to TRC40 (Mariappan et al., 2010, Nature, 466:1120-4). By contrast, PrP crosslinking to TRC40 was minimal, with Bag6 being the primary interacting partner.

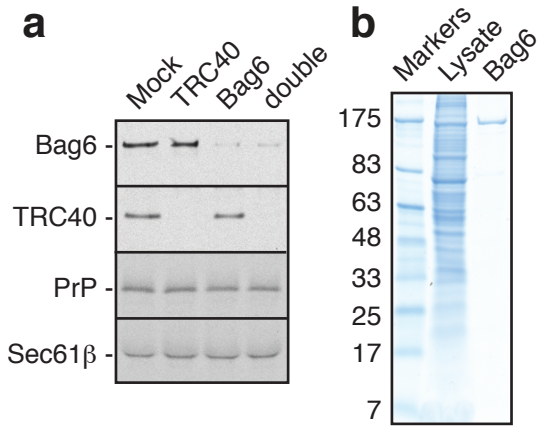

Sup. Fig. S16. Bag6 depletion and purification. (a) RRL was subjected to immunodepletion using antibodies to GFP ('Mock'), TRC40, Bag6, or both TRC40 and Bag6 ('double'). Equal aliquots of the depleted lysates were analyzed by immunoblotting against TRC40 and Bag6. Depletion of TRC40 was ~90% and Bag6 ~80%. Note that upon Bag6 depletion, Ubl4A and TRC35 are comparably depleted (Mariappan et al., 2010, Nature, 466:1120-4). In addition, the four lysates were used for in vitro translation of PrP and Sec61β to illustrate no effect on protein synthesis. Translation time was 30 min. (b) FLAG-tagged Bag6 was purified from overexpressing HEK-293T cells and analyzed by colloidal coomassie blue staining. A version lacking the Ubl domain was purified the same way with identical yield and purity (not shown).

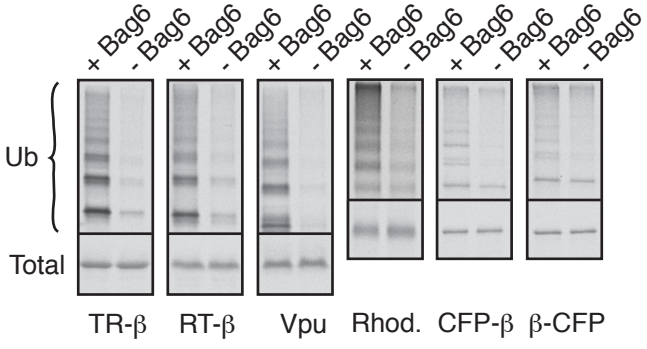

Sup. Fig. S17. Various MLPs are dependent on Bag6 for efficient ubiquitination. RRL containing or depleted of Bag6 complex was used for translations of the indicated proteins. Translation reactions contained 10 uM His-Ub, and were incubated for 1 h. Ubiquitinated products were captured using immobilized Co^{+2} (upper panels). An aliquot of total translation was also analyzed to confirm equal synthesis (bottom panels). CFP-β and β-CFP are constructs in which Sec61β was appended with CFP at the N- or C-terminus, respectively. Thus, β-CFP contains an internal TM domain, while CFP-β remains a tail-anchored protein.

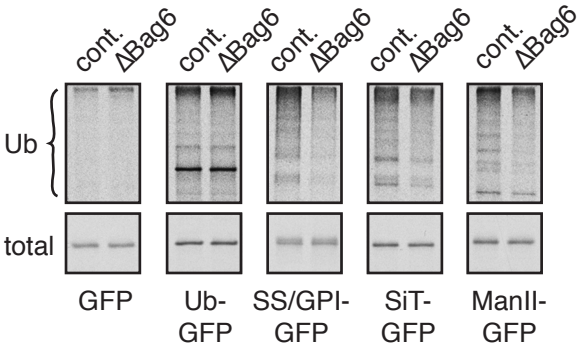

Sup. Fig. S18. The Bag6 complex facilitates ubiquitination via hydrophobic domains. GFP or versions appended with the indicated domains were translated in vitro using lysates subjected to control or Bag6 immunodepletion. 10 uM His-ubiquitin was included in the reactions. The isolated ubiquitinated products (top panels) and an aliquot of total translation products (bottom panels) are shown. Note that Bag6 depletion influences ubiquitination selectively of constructs containing hydrophobic domains. Ub-GFP is a linear fusion of Ubiquitin and GFP.

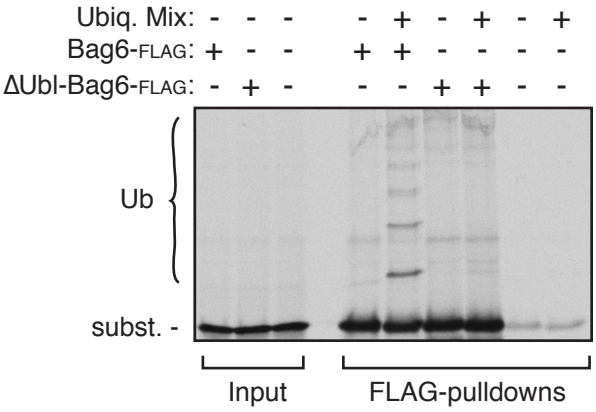

Sup. Fig. S19. The Bag6 complex recruits ubiquitination machinery via its Ubl domain. TR-β was translated in Fr-RRL supplemented with FLAG-tagged recombinant Bag6, ΔUbl-Bag6, or buffer. In the Fr-RRL system, substrate is not ubiquitinated due to lack of ubiquitin and UbcH5. The sample was affinity purified via the FLAG tag and incubated with or without a ubiquitination mix (20 uM His-ubiquitin, 100 nM E1, 250 nM UbcH5a, and energy regenerating system). An aliquot of the input translation shows equal substrate synthesis. Both Bag6 and ΔUbl-Bag6 effectively capture substrate, but only the former becomes ubiquitinated (verified by ubiquitin pulldowns; not shown).

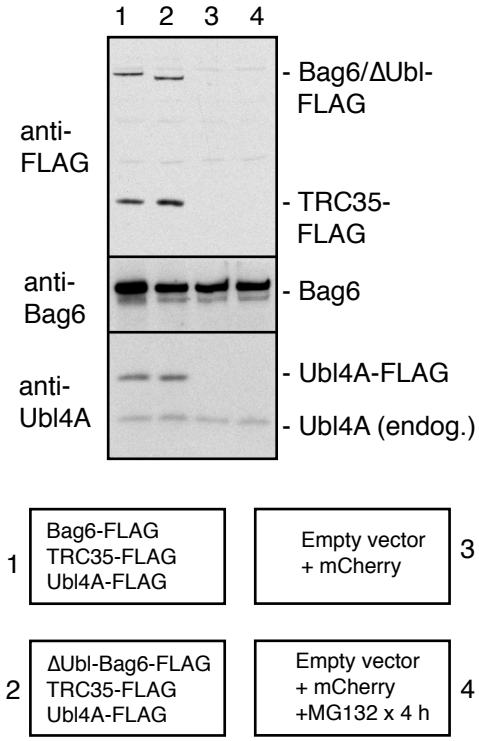

Sup. Fig. S20. Characterization of Bag6 complex expression. Mouse N2a cells in a 24-well dish were transfected with a mixture of expression plasmids for Bag6-FLAG (425 ng), TRC35-FLAG (225 ng), Ubl4A-FLAG (50 ng) and a PrP construct (100 ng). Preliminary experiments established the relative ratios that gave roughly equal expression levels of each Bag6 complex subunit. Lane 2 contained ΔUbl-Bag6-FLAG instead of Bag6-FLAG. Lanes 3 and 4 contained an empty vector (600 ng) and 100 ng mCherry expression vector in lieu of Bag6 complex plasmids. At 20 h, MG132 was added to 10 uM to the fourth sample, and all samples harvested at 24 h. Shown are blots for the FLAG tag, Bag6 and Ubl4A. The Bag6 and Ubl4A blots show that the exogenous proteins are expressed ~2X that of endogenous proteins. TRC35 could not be assessed similarly because the C-terminal antibody epitope is obscured by the FLAG tag, although we presume its levels are similar to Bag6-FLAG based on the FLAG blot. Note that ΔUbl-Bag6-FLAG is not detected by the Bag6 antibody, whose antigen includes the deleted domain, but its expression level was confirmed by the FLAG blot to be equal to Bag6-FLAG. This same ratio of Bag6 complex proteins was used in Fig. 4f, 4g, and Sup. Fig. S18. PrP expressed in these cells was of Hamster origin, and can be detected specifically using the 3F4 antibody. The endogenous Ubl4A serves as a convenient loading control in these experiments.

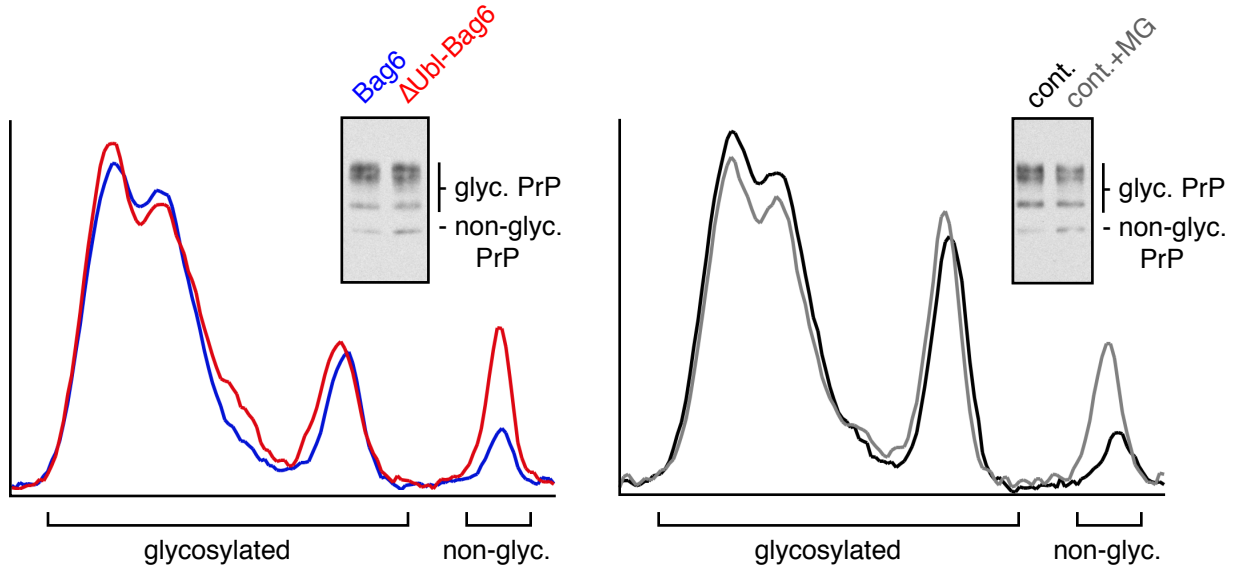

Sup. Fig. S21. Quantification of PrP stabilization by ΔUbl-Bag6 dominant negative expression. Mouse N2a cells in a 24-well dish were transfected with wild type PrP and either the Bag6 complex, ΔUbl-Bag6 complex, or control vectors, as in Sup. Fig. S20. The samples were harvested and immunoblotted to detect PrP (insets). The glycosylation pattern is a characteristically heterogeneous mixture of core and complex glycans, unlike the simpler in vitro translated product (e.g., Fig. 1) which only recieves core glycans. The graphs show a normalized densitometry scan down each lane, color coded as indicated. Note that ΔUbl-Bag6 complex expression leads to a ~2-fold selective increase in non-glycosylated PrP (left panel). The same level of increase is observed with 2 h proteasome inhibition on samples analyzed in parallel (right panel). Note also that there is a slight change in the glycoform pattern upon overexpression of either the Bag6 complex or Δ Ubl-Bag6 complex. This is probably due to indirect effects on vesicular trafficking secondary to slight differences in SNARE levels, given that Bag6 complex is involved in their insertion. Similar subtle changes in glycoforms were observed (in the opposite direction) upon shRNA-mediated silencing of Bag6 (see Sup. Fig. S22). Importantly however, these effects were not dependent on the Ubl domain of Bag6, consistent with this domain being dispensible for the chaperoning activity of Bag6 involved in its TA insertion functions. Finally, we have observed that even wild type Bag6 complex can have a dominant-negative effect if the ratio of its subunits are not roughly equal. This is seen to a slight degree in Fig. 4d, where the translocation-deficient PrP construct is stabilized partially by wild type Bag6 complex.

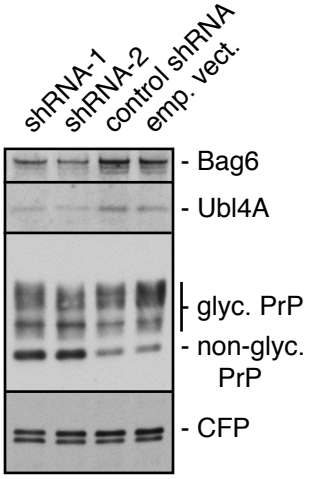

Sup. Fig. S22. Effect of Bag6 silencing on PrP. Hela cells were co-transfected with expression plasmids for PrP, CFP, and one of two different shRNAs against human Bag6. As controls, an irrelevant shRNA and the empty shRNA vector were used. After 103 h, the cells were harvested and analyzed by immunoblotting against the indicated proteins. Note that Bag6 (and the associated Ubl4A) were reduced ~50% by the shRNA treatment. This had minimal effect on CFP expression levels, but led to a selective stabilization of non-glycosylated PrP. The basis of the two bands for CFP is not clear, but may be due to alternative start codon usage or some degradation given that non-native residues are appended to CFP via translation through the polylinker of this empty plasmid. The non-glycosylated species is due to inefficient translocation since it is not observed upon increasing signal sequence efficiency (e.g., Fig. 4e). The slightly different glycosylation patterns between this and other experiments (e.g., Fig. 4e, Sup. Fig. S21) are due to cell type specific differences.

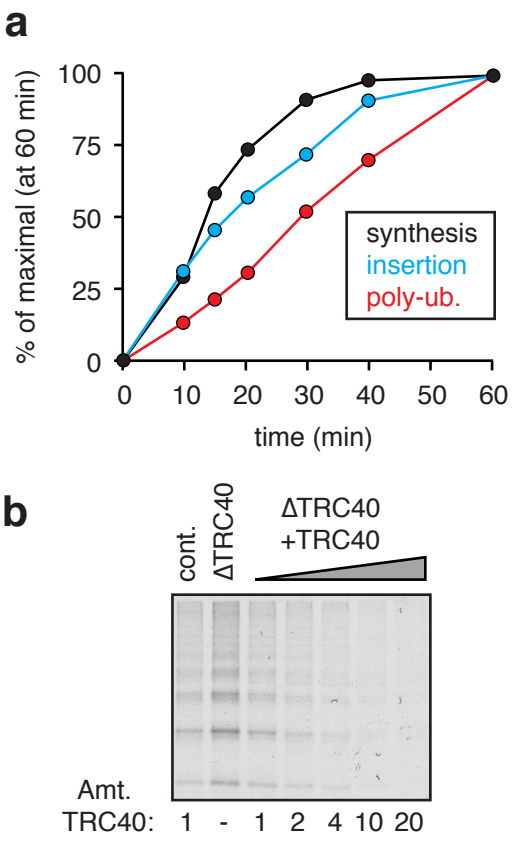

Sup. Fig. S23. Analysis of Sec61β ubiquitination. (a) Sec61β was translated in RRL supplemented with 10 uM His-Ub for 1 h. One reaction contained RMs, while another did not. The reaction containing RMs was assayed at various time points for membrane insertion using a protease-protection assay (Stefanovic and Hegde, 2007, Cell, 128:1147-59). The reaction lacking RMs was assayed at various time points for ubiquitination by pulldowns with immobilized Co^{+2}. The relative amounts (normalized to the 60 min value) of synthesis, insertion, and ubiquitination were quantified and plotted. Note that insertion is very closely timed with synthesis, while ubiquitination is slower and lags at least 10 min behind synthesis. (b) Sec61β was translated in RRL that was mock-depleted ('cont.'), TRC40-depleted, or TRC40-depleted and replenished to various levels with recombinant zebrafish TRC40. All reactions contained His-ubiquitin at 10 uM. The ubiquitinated products of each reaction were captured with immobilized Co^{+2} and analyzed. The amount of TRC40 in each reaction is indicated, relative to that in RRL.